



# Estimation of Strength Development on Solidified Soft Soil Using Bender Elements and X-ray CT Scan Technique

Enkhzaya Batbayar<sup>1</sup>, Takayuki Kawaguchi<sup>2\*</sup> and Dai Nakamura<sup>2</sup>

<sup>1</sup>Division of Project control, Barilga JCS, Ulaanbaatar, Mongolia

<sup>2</sup>Division of Civil and Environmental Engineering, Kitami Institute of Technology, Hokkaido, Japan

\*Corresponding author: [kawa@mail.kitami-it.ac.jp](mailto:kawa@mail.kitami-it.ac.jp)

**Abstract.** Cement, which can solidify soft soil, not only improves the bearing capacity of poor ground but also contributes to solving various ground environmental issues, including the containment of pollutants. In this regard, the amount of cement added to the soil to achieve the required strength on the construction site is determined based on the results of unconfined compression tests with numerous test specimens. However, due to significant variability in the unconfined compression strength of solidified soil specimens, a considerable safety factor is applied to the strength, resulting in a substantial excess of cement being added compared to the amount necessary to obtain the desired strength. Furthermore, because laboratory tests to determine the amount of cement to be added require a considerable amount of time, there are cases where an empirical approach is used, adding more cement than necessary without conducting laboratory tests. As cement production releases a large amount of carbon dioxide, accurately predicting the unconfined compression strength of cement-improved soil after sufficient curing from short-term tests can not only reduce construction costs but also mitigate the environmental impact. Therefore, in this study, we focused on accurately and rapidly predicting the future strength used in the design of soil structures using two non-destructive tests. As a result, we successfully predicted the future unconfined compression strength using the shear wave velocity obtained from bender element tests. Furthermore, X-ray CT scanning was found to be a valuable test as it not only visualizes the interior of the test specimen but also allows for the assessment of density increase associated with curing, which contributes to the validation of the obtained unconfined compression strength.

**Keywords:** Solidified soil, Non-destructive test, Geoenvironmental problem.

## 1 Introduction

By adding cement or other solidifying agents to soft clayey soils with high water content, such as dredged soil, they can be recycled as high-quality geomaterials [1].

© The Author(s) 2023

O. Batdelger et al. (eds.), *Proceedings of the Fourth International Conference on Environmental Science and Technology (EST 2023)*, Advances in Engineering Research 224,

[https://doi.org/10.2991/978-94-6463-278-1\\_16](https://doi.org/10.2991/978-94-6463-278-1_16)

Additionally, constructing improvement columns that mix soil and stabilizer in the ground enables addressing geoenvironmental problems, such as containment of pollutants [2]. In such cases, the amount of stabilizer added to the soil to achieve the required strength on the construction site is determined through unconfined compression test results conducted in the laboratory on numerous specimens with varying amounts of the agent and different curing periods. However, due to the significant variation in unconfined compression strength of the solidified soil specimens [3], safety factors are set considerably high, resulting in the addition of a considerably larger amount of stabilizer than necessary to attain the required strength. Moreover, laboratory tests to determine the appropriate amount of stabilizer require a substantial amount of time. In situations where there is limited time for mixed design, laboratory tests may not be feasible, and large safety factors are employed based on empirical prediction methods, leading to the addition of more stabilizer. Cement, the most commonly used stabilizer, emits a significant amount of carbon dioxide during its production process. Therefore, accurately predicting the strength of cement-solidified soil in a short period would allow for the reduction of cement used, resulting in cost savings and mitigating environmental impacts.

In this study, we aimed to establish a method for accurately predicting the future unconfined compression strength of cement-treated soil specimens using the bender element test over a short timeframe. The bender element is a piezoelectric element coated with insulation and waterproofing, inserted into the ends of the soil specimens [4]. By applying voltage waveforms to the bender element at the soil specimen's end, we can easily measure the shear wave velocity propagating within the soil. The method allows us to precisely estimate the unconfined compression strength at later time points (e.g., 28 days or 91 days after cement addition), which is essential for designing soil structures, based on the rate of shear wave velocity increase observed during the first few days after cement addition.

Furthermore, we verified whether X-ray CT scanning [5], another non-destructive test, could not only visualize the voids inside the specimens, which is one of the causes of strength variation, but also determine the increase in density associated with the hardening required for predicting unconfined compression strength. Additionally, the results obtained from this research are expected to be applicable not only to cement but also to other solidifying agents with low carbon dioxide emissions that are added to soil [6, 7].

## 2 Method

### *Test Specimens*

Table 1 summarizes the test conditions conducted in this study. Two types of dredged soils retrieved from Tokyo Bay (soil particle density,  $\rho_s=2.62\text{ g/cm}^3$ , liquid limit,  $w_L=104\%$ ) and Nagoya Port ( $\rho_s=2.69\text{ g/cm}^3$ ,  $w_L=66\%$ ) were used in the tests. Both soils were adjusted to approximately 1.3 times  $w_L$  and mixed with ordinary

Portland cement at a ratio of 100 kg/m<sup>3</sup>. After mixing for 10 minutes in a mixer, the specimens were cured.

**Table 1.** Summary of test conditions

**Tokyo Bay**

| Tests | Cement content (g/m <sup>3</sup> ) | Initial water content (%) | Curing days | Curing method | BE test |
|-------|------------------------------------|---------------------------|-------------|---------------|---------|
| B1 T  | 100                                | 135                       | 3           | B             | No      |
| B2 T  |                                    |                           | 7           |               |         |
| B3 T  |                                    |                           |             |               |         |
| B4 T  |                                    |                           |             |               |         |
| B5 T  |                                    |                           |             |               |         |
| B6 T  |                                    |                           |             |               |         |
| B7 T  |                                    |                           |             |               |         |
| B8 T  |                                    |                           |             |               |         |
| B9 T  |                                    |                           |             |               |         |
| B10 T |                                    |                           |             |               |         |
| K1 T  | 100                                | 135                       | 3           | K             | Yes     |
| K2 T  |                                    |                           | 7           |               |         |
| K3 T  |                                    |                           | 14          |               |         |
| K4 T  |                                    |                           | 28          |               |         |
| K5 T  |                                    |                           | 91          |               |         |
| K6 T  |                                    |                           | 91          |               |         |
| S1 T  | 100                                | 135                       | 3           | S             | Yes     |
| S2 T  |                                    |                           | 7           |               |         |
| S3 T  |                                    |                           | 14          |               |         |
| S4 T  |                                    |                           | 28          |               |         |

**Nagoya Port**

|      |     |    |    |   |     |
|------|-----|----|----|---|-----|
| B1 N | 100 | 89 | 3  | B | No  |
| B2 N |     |    | 7  |   |     |
| B3 N |     |    |    |   |     |
| B4 N |     |    |    |   |     |
| B5 N |     |    |    |   |     |
| B6 N |     |    |    |   |     |
| B7 N |     |    |    |   |     |
| B8 N |     |    |    |   |     |
| K1 N | 100 | 89 | 3  | K | Yes |
| K2 N |     |    | 7  |   |     |
| K3 N |     |    | 14 |   |     |
| K4 N |     |    | 28 |   |     |
| S1 N | 100 | 89 | 3  | S | Yes |
| S2 N |     |    | 7  |   |     |
| S3 N |     |    | 14 |   |     |
| S4 N |     |    | 28 |   |     |

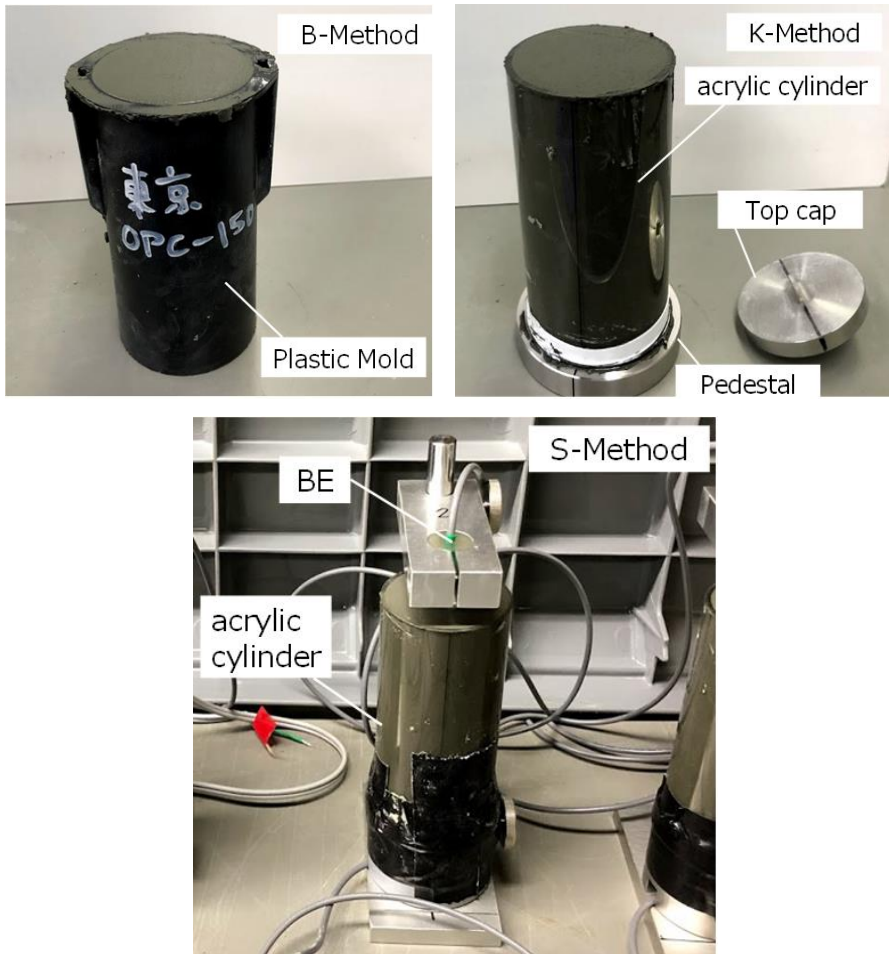


**Photo 1.** Curing method of soil specimens

Photo 1 shows three different curing methods. The specimens that did not conduct Bender Element (BE) tests were filled into demouldable plastic molds, covered with a wrap at the top, and cured inside a high humidity container (B-Method). Some of the specimens that conducted BE tests were filled into transparent acrylic cylinders, and a top cap with protrusions to create a cavity of the same shape as the BEs, along with a pedestal, was installed (K-Method). These specimens were then cured inside the aforementioned container. The remaining specimens that conducted BE tests were filled into transparent acrylic cylinders and kept in place with the apparatus equipped with the BEs (S-Method). They were also cured inside a high humidity container.

#### *Bender Element Tests*

Photo 2 shows the BE testing system. The transmitter BE is inserted at the upper end of the specimen. When a voltage waveform signal of one wavelength is applied to the transmitter BE from the function generator, it vibrates, and this vibration propagates through the specimen to the receiver BE, which is inserted at the lower end of the specimen. The voltage applied to the transmitter BE and the voltage generated by the vibration of the receiver BE are recorded using a digital storage oscilloscope.

Fig. 1 presents an example of the BE test results. The shear wave velocity,  $V_s$ , was calculated from the travel time  $\Delta t$  and travel distance,  $L$ , determined from the transmitted and received voltage waveforms ( $V_s = \Delta t / L$ ). It can be observed that as the curing days increase, the time taken for shear waves to propagate decreases. The arrival time of the shear wave was determined following the method proposed by [8]. The elastic shear modulus,  $G$ , was calculated from the wet density,  $\rho$ , of the soil specimen and the  $V_s$  ( $G = \rho V_s^2$ ).

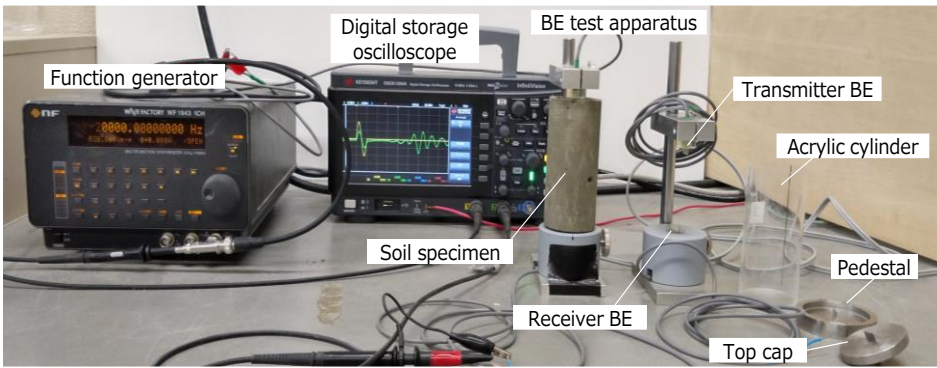


Photo 2. BE test system

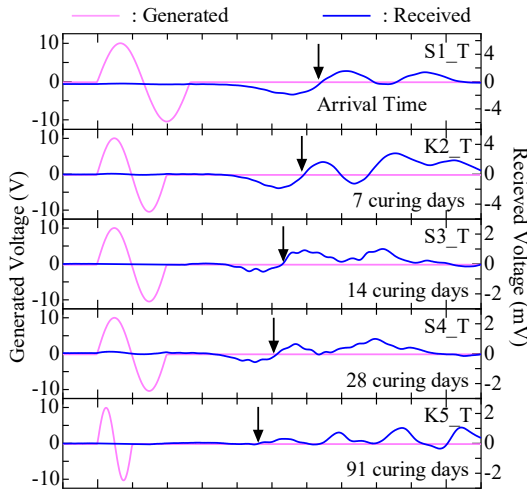
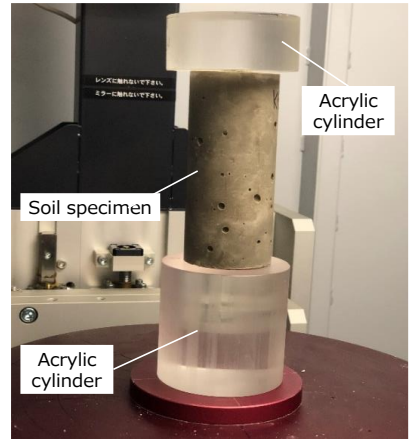
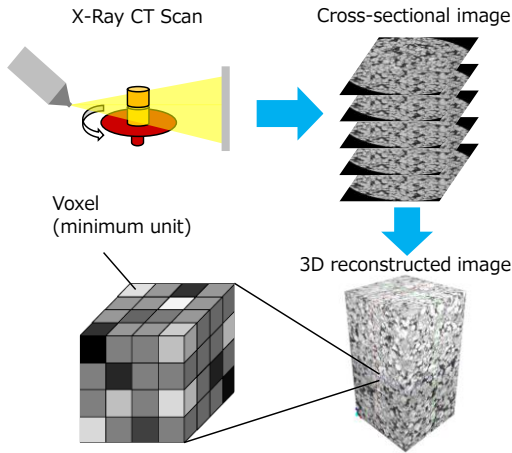


Fig. 1. Example of BE test results

### *X-ray CT scan*

Fig. 2 is a schematic diagram illustrating the data acquisition process of the microfocus X-ray CT scanning device used in this study. The object of interest is divided into small cubes (voxels), and the average X-ray absorption value of each voxel is outputted as the gray level (GL) value. It should be noted that the GL value is proportional to the density of the object.

Photo 3 shows a soil specimen installed in the X-ray CT device. Since the GL value is a relative indicator, a uniform acrylic cylinder with known density was scanned together with the soil specimen for reference.



**Fig. 2.** Data acquisition process of the X-ray CT

**Photo 3.** Soil specimen installed in the X-ray CT device

## 3 Result and Discussion

Fig. 3 shows the variation of unconfined compressive strength,  $q_u$ , and shear wave velocity,  $V_s$ , with curing days for the specimens made by mixing cement to the dredged

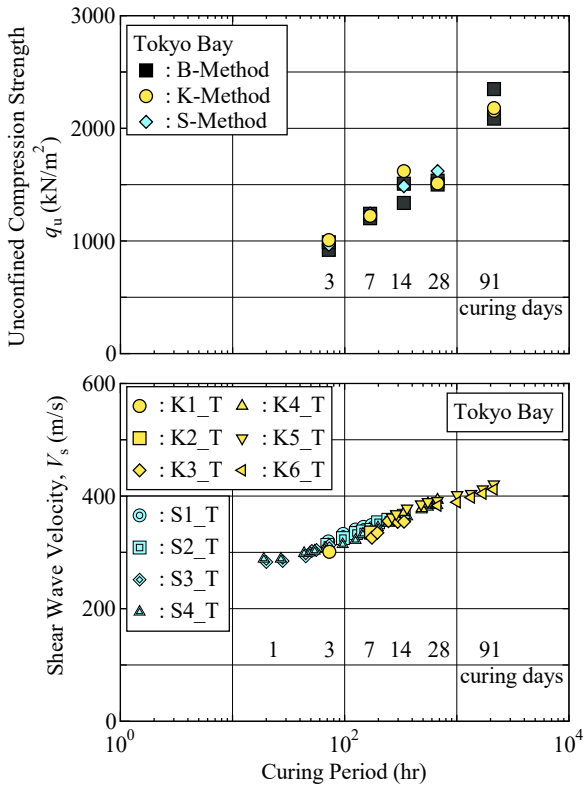


**Fig. 3.** Variation of  $q_u$ , and  $V_s$  with curing days

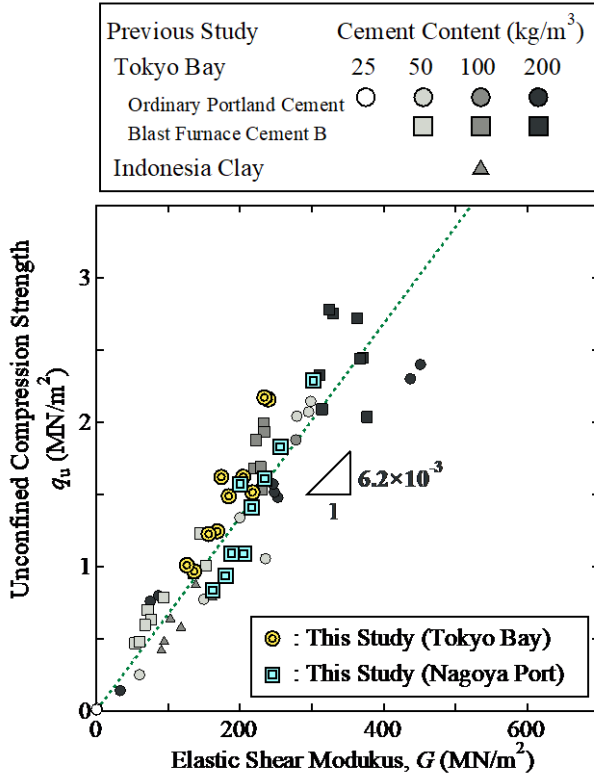


Fig. 4. Relationship between  $q_u$  and  $G$

soil retrieved from Tokyo Bay. Both relationships can be observed to increase linearly with curing days on a logarithmic scale graph. In particular, it has been found that the  $V_s$  can be measured even at curing days as early as one day, when the specimen is not fully solidified. Furthermore, it is possible to predict the  $V_s$  at 28 days and 91 days without destroying the specimen by unconfined compression tests.

Fig. 4 represents the relationship between  $q_u$  and the elastic shear modulus,  $G$ , calculated from the  $V_s$  using bender element (BE) test. This figure includes the results of previous study using specimens made by solidifying different clays with cement and specimens made with different cement contents. The proportional relationship between the  $q_u$  and  $G$  in cement-treated soil has been reported in other studies as well [9]. However, it is evident from this figure that the relationship between  $q_u$  and  $G$  can be generally expressed by the same proportional equation, regardless of the kind of based clay or the cement addition rates. Therefore, by utilizing these relationships, it should be possible to accurately estimate future unconfined compression strength based on the variations in shear wave velocity measured from small amount of soil specimens with added stabilizer.

Fig. 5 provides an example of X-ray CT scan results for the soil specimen solidified with cement, which were used in this study. It clearly shows the indentations of the



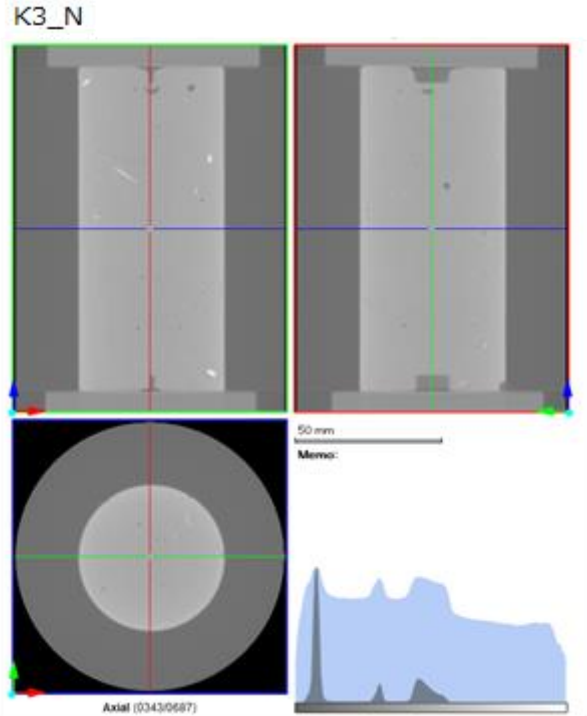


**Fig. 5.** Example of X-ray CT scan result

bender elements and the presence of air bubbles within the specimen. Furthermore, the histogram in the bottom right represents the gray level (GL) values, showing three distinct peaks corresponding to air, acrylic, and the soil specimen itself.

Fig. 6 compares the histograms of the GL values for specimens with different curing days made from dredged clay retrieved from Tokyo Bay. The horizontal axis of this figure is normalized such that the first peak corresponds to air density ( $0.00 \text{ g/cm}^3$ ) and the second peak corresponds to acrylic density ( $1.19 \text{ g/cm}^3$ ). Additionally, the vertical axis is also normalized to compensate for the volume differences among the soil specimens. When zooming in on the third peak corresponding to the soil specimens, it was observed that as the curing days increased and the unconfined compressive strength of the specimens increased, the peak became higher and shifted to the right. Based on these findings, it can be concluded that X-ray CT scan images and histograms of GL values are effective techniques for quality evaluation of solidified soil specimens.

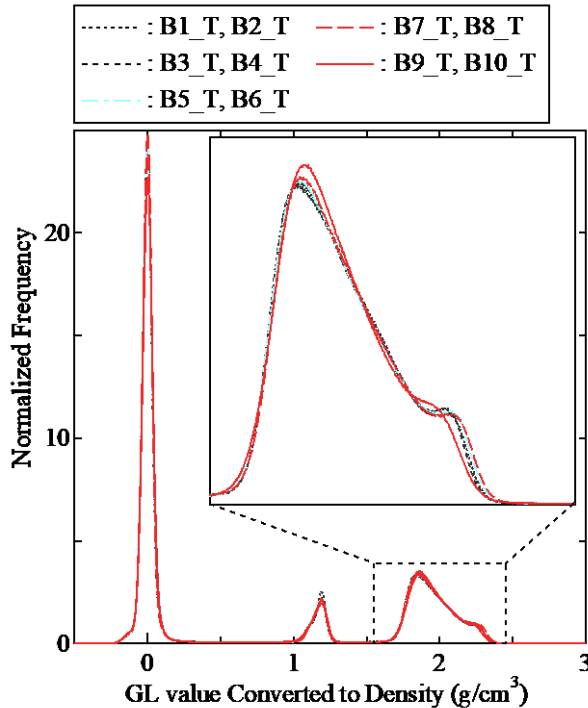


Fig. 6. Histograms of the GL values for specimens with different curing days

## 4 Conclusions

From numerous bender element tests and unconfined compression test results using dredged clayey soil with added cement, it was observed on a logarithmic graph that the shear wave velocity increases linearly with curing days. Therefore, it was revealed that the unconfined compression strength at 28 days and 91 days can be accurately estimated based on the variation in shear velocity during a short curing period of about 3 to 7 days by using the proportional relationship between the elastic shear modulus calculated from shear wave velocity and the unconfined compression strength.

By utilizing this achievement, it will be possible to reduce the usage of cement, which releases a large amount of carbon dioxide during its production. As a result, in the future, it is expected to lead to a reduction in environmental impact and cutting down construction costs.

It has been discovered that there is a correlation between the peak of the Gray Level (GL) values obtained from X-ray CT scans and the unconfined compression strength of the solidified soil specimens. Therefore, X-ray CT scanning not only helps to identify the location and size of air bubbles that may negatively affect the unconfined compression strength, but also assists in predicting the inherent strength that was supposed to be demonstrated.

As a result, it is recommended to perform X-ray CT scanning before conducting unconfined compression tests on soil specimens with added stabilizer in the future. By doing so, it will undoubtedly facilitate the quality assessment of solidified soil specimens and the interpretation of unconfined compression test results with significant variations.

## References

1. Kitazume, M., Yoshin, N., Shinsha, H., Horii, R. and Fujio, Y.: Field test on pneumatic flow mixing method for sea reclamation, *Proc. of Coastal Geotechnical Engineering in Practice* 1:647-652 (2000).
2. Kamon, M.: Remediation techniques by use of ground improvement, *Soft Ground Technology*, J.L. Hanson and R.J. Termaat, (eds), ASCE: 374-387 (2001). [https://doi.org/10.1061/40552\(301\)29](https://doi.org/10.1061/40552(301)29)
3. Sawa, K., Nakayama, Y., Kusumoto, N. and Nakata, Y.: About the uncertainty of unconfined compression test results of cement improved soil, *Proc. of the 10th National Symposium on Ground Improvement, JSMS*: 181-188 (2012).
4. Dyvic, R. and Madhsus, C.: Laboratory measurements of G using bender elements. *Proc. of the ASCE annual convention, Detroit*: 186-196 (1985).
5. Otani, J., Mukunoki, T. and Sugawara, K.: Evaluation of particle crushing in soils using X-ray CT data. *Soils and Foundations* 45(1): 99-108 (2005).
6. Tanaka, Y., Hamatani, S., Nonaka, S. and Nakagawa, M.: Estimate of CO<sub>2</sub> emissions during construction of steel slag-dredged soil mixture and examination of reduction method. *Journal of Japan Society of Civil Engineers B3* 78(2): I\_157-I\_162 (2022). [https://doi.org/10.2208/jscejoe.78.2\\_I\\_157](https://doi.org/10.2208/jscejoe.78.2_I_157)
7. Imran, M.A., Nakashima, K., Evelpidou, N. and Kawasaki, S. 2022. Durability improvement of biocemented sand by fiber-reinforced MICP for coastal erosion protection, *Materials* 15(7): 2389 (2022). <https://doi.org/10.3390/ma15072389>
8. Kawaguchi, T., Ogino, T., Yamashita, S. and Kawajiri, S.: Identification method for travel time based on the time domain technique in bender element tests on sandy and clayey soils. *Soils and Foundations* 56(5): 937-946 (2016). <https://doi.org/10.1016/j.sandf.2016.08.017>
9. Shibuya, S., Mitachi, T. and Ozawa, H.: Time/stress-history dependency of deformation-strength characteristics of cement-mixed sand. *Journal of Japan Society of Civil Engineers*, 687: 249-257 (2001). [https://doi.org/10.2208/jscej.2001.687\\_249](https://doi.org/10.2208/jscej.2001.687_249)

**Open Access** This chapter is licensed under the terms of the Creative Commons Attribution-NonCommercial 4.0 International License (<http://creativecommons.org/licenses/by-nc/4.0/>), which permits any noncommercial use, sharing, adaptation, distribution and reproduction in any medium or format, as long as you give appropriate credit to the original author(s) and the source, provide a link to the Creative Commons license and indicate if changes were made.

The images or other third party material in this chapter are included in the chapter's Creative Commons license, unless indicated otherwise in a credit line to the material. If material is not included in the chapter's Creative Commons license and your intended use is not permitted by statutory regulation or exceeds the permitted use, you will need to obtain permission directly from the copyright holder.

